flashes were compensated for with fresh NP-EGTA and $CaCl_2$.

18. The time course and magnitude of the change in [Ca^{2+}] could be modified by varying the frequency and the discharge energy of the Q-switched, frequency-tripled, neodymium-doped:yttrium-aluminum-garnet (Nd:YAG) laser (model GCR-18, Spectra-Physics, Mountain View, CA). Ultraviolet light (352 nm) from the laser was separated from the 1064 and 532 lines with three dichroic mirrors (350 to 360 nm), collected by a convergent mirror, and focused onto the polished aperture of a ~400-μm outer diameter, fused-silica light guide (Fiberguide, Stirling, NJ). The end of the light guide was positioned with a micromanipulator ~400 μm in front of the bilayer aperture to photolyze the caged Ca^{2+} in a cylinder-shaped region between the end of the fiber optic light guide and the bilayer cup. Slow changes in [Ca^{2+}] ("Ca^{2+} ramps") were produced by setting a low output energy of the flash lamp (5 to 15 mJ) and pulsing the laser at 10 Hz. Fast [Ca^{2+}] changes (~100 μs, the rate time constant of Ca^{2+} release by NP-EGTA) were produced by 50- to 80-mJ single flashes. All flashes were ~7 ns in duration. We measured the local changes in [Ca^{2+}] by two methods. In one case, small (50- to 70-μm tip diameter) plastic pipettes were filled with a Ca^{2+} ionophore resin (catalogue no. 21199, Fluka Chemical, New York, NY) and positioned in the path of the light beam, ~200 μm away from the bilayer surface. In the second case, the bilayer aperture was filled with the Ca^{2+} ionophore resin as described (*14*), and the change in [Ca^{2+}] was determined in separate experiments. Both methods yielded very similar results.
19. H. H. Valdivia, J. H. Kaplan, G. C. R. Ellis-Davies, W. J. Lederer, unpublished data.
20. D. Bers, *Am J. Physiol.* **256**, C109 (1989); I. Baró *et al.*, *J. Physiol. (London)* **465**, 21 (1993).
21. W. J. Lederer *et al.*, *Science* **251**, 1371 (1990).
22. P. J. O'Brien, *Can. J. Vet. Res.* **50**, 318 (1986).
23. E. Rousseau *et al.*, *Biophys. J.* **50**, 1009 (1986).
24. G. Callewaert, L. Cleeman, M. Morad, *Proc. Natl. Acad. Sci. U.S.A.* **85**, 2009 (1988); H. A. Spurgeon *et al.*, *Am. J. Physiol.* **258**, H574 (1990).
25. The catalytic subunit of PKA (Sigma Chemical, St. Louis, MO) was activated before use with 0.5 M dithiothreitol (DTT) for 30 min at 32°C and dialyzed for 4 hours at 4°C against the cis solution with 1 mM DTT (*30*). PKA was added directly to the cis solution supplemented with 1 mM MgATP, and the RyR activity was recorded 1 to 2 min after addition. The binding of [^{3}H]ryanodine (7 nM) to porcine cardiac SR vesicles (0.3 mg/ml) was done for 90 min at 36°C in 0.2 M KCl, 10 mM Na-Pipes (pH 7.2), 1 mM MgATP, and 10 μM $CaCl_2$, as described (*28, 29*).
26. Similar to ATP, the addition of 3 mM AMP-PCP to the cis (cytosolic) side of the channel increased the peak P_o and the plateau P_o of single RyRs activated by a fast change in [Ca^{2+}] from 0.1 to 10 μM in the presence of 4 mM $MgCl_2$. This suggested that AMP-PCP was as effective as ATP to directly activate RyRs (*9*), decrease the concentration of free Mg^{2+}, or both. However, in two experiments, AMP-PCP–treated RyRs did not change significantly peak P_o (0.68, 0.71), τ_{adapt} (196, 173 ms), and plateau P_o (0.29, 0.32) when recorded in the absence and the presence, respectively, of PKA (1 μg/ml).
27. S. C. O'Neill, J. G. Mill, D. Eisner, *Am. J. Physiol.* **258**, C1165 (1990).
28. H. H. Valdivia *et al.*, *J. Biol. Chem.* **266**, 19135 (1991).
29. H. H. Valdivia, M. Kirby, W. J. Lederer, R. Coronado, *Proc. Natl. Acad. Sci. U.S.A.* **89**, 12185 (1992).
30. A. Yatani *et al.*, *J. Biol. Chem.* **263**, 9887 (1988).

31. We thank M. Fill for his help with the experimental setup modeled on his own (*14*), M. Kirby for help with the Ca^{2+} electrode, and M. Fill, G. Meissner, I. Pessah, and E. Ríos for critical comments on this manuscript. Supported by a Grant-in-Aid from the American Heart Association (AHA) to H.H.V., NIH grants HL36974 and HL25675 (to W.J.L.) and HL30315 and GM39500 (to J.H.K.). H.H.V. is a recipient of a Minority Scientist Development Award from the AHA.

13 September 1994; accepted 13 December 1994

Altered Cytokine Export and Apoptosis in Mice Deficient in Interleukin-1β Converting Enzyme

Keisuke Kuida, Judith A. Lippke, George Ku, Matthew W. Harding, David J. Livingston, Michael S.-S. Su,* Richard A. Flavell*

The interleukin-1β (IL-1β) converting enzyme (ICE) processes the inactive IL-1β precursor to the proinflammatory cytokine. Adherent monocytes from mice harboring a disrupted ICE gene ($ICE^{-/-}$) did not export IL-1β or interleukin-1α (IL-1α) after stimulation with lipopolysaccharide. Export of tumor necrosis factor–α and interleukin-6 (IL-6) from these cells was also diminished. Thymocytes from $ICE^{-/-}$ mice were sensitive to apoptosis induced by dexamethasone or ionizing radiation, but were resistant to apoptosis induced by Fas antibody. Despite this defect in apoptosis, $ICE^{-/-}$ mice proceed normally through development.

The cytokine IL-1β plays a pivotal role in acute and chronic inflammation, bone resorption, myelogenous leukemia, and other pathological processes (*1*). IL-1β is synthesized as a 31-kD precursor devoid of a conventional signal sequence (*2*) and is processed to its proinflammatory 17-kD form by ICE, a cysteine protease with substrate cleavage specificity for Asp-X (*3*). ICE itself is synthesized principally in monocytes as an inactive proenzyme that autoprocesses to an active tetramer composed of two 10-kD and two 20-kD subunits (*4, 5*). With the cloning of the *Caenorhabditis elegans* cell death gene *ced-3* (*6*), ICE was recognized to be a member of a new subfamily of cysteine proteases. ICE and CED-3 show only 28% sequence conservation overall, but their active site residues are completely conserved (*5, 6*).

Although the physiological functions of the mammalian ICE homologs are unknown, overexpression of ICE and ICE homologs in transfected cell lines induces apoptosis (*7, 8*). This effect is reduced when ICE is coexpressed with Bcl-2, a mammalian oncogenic protein that is a general suppressor of apoptosis (*9*). Further, transfection of chicken dorsal ganglion cells with CrmA, a serpin-like inhibitor of ICE (*10*) and potentially of ICE homologs, protects these cells from apoptosis induced by depletion of nerve growth factor (*11*).

To probe the physiological functions of ICE, we disrupted the murine ICE gene in D3 embryonic stem (ES) cells by replacing part of exons 6 and 7 (Fig. 1A) with a neomycin resistance gene cassette (*12, 13*). Chimeric mice were obtained by injection of mutant ES cells into C57BL/6 blastocysts, and the chimeric males were mated with C57BL/6 mice. Interbreeding of the heterozygous mice generated the expected mendelian 1:2:1 ratio of wild-type ($ICE^{+/+}$), heterozygous ($ICE^{+/-}$), and homozygous ($ICE^{-/-}$) mutant mice. Homozygous mice with two copies of the disrupted ICE gene

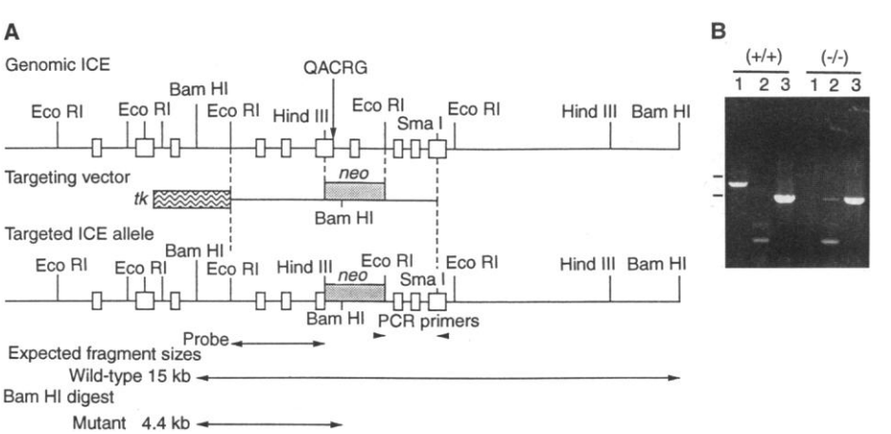

Fig. 1. Disruption of the murine ICE gene by homologous recombination (*13*). (**A**) Restriction maps of the murine ICE locus, the targeting vector, and the mutant ICE locus. (**B**) RT-PCR analysis of mRNA from $ICE^{+/+}$ and $ICE^{-/-}$ mice with oligonucleotide primers (*13*) specific for wild-type ICE cDNA (1), mutated ICE cDNA (2), and β-actin cDNA (3). The lines on the left indicate the positions of 984-bp (upper) and 738-bp (lower) markers.

were identified by Southern blots of genomic DNA, and the absence of ICE mRNA in $ICE^{-/-}$ mice was confirmed by reverse transcription–polymerase chain reaction (RT-PCR) analysis (Fig. 1B). The $ICE^{-/-}$ mice were healthy and fertile, and had no gross abnormalities in appearance, body weight, or organ size for at least the first 16 weeks of life. The apparently normal phenotype of $ICE^{-/-}$ mice suggests that ICE expression is dispensable for development.

Several serine proteases can process the IL-1β precursor to bioactive forms (*14*), but ICE is the only mammalian protease identified that generates the mature 17-kD cytokine with the naturally occurring Ala^{118} amino-terminus (*3*). A tetrapeptide inhibitor of ICE [Ac-Tyr-Val-Ala-Asp-CHO; inhibition constant (K_i) = 0.7 nM] blocks IL-1β processing and secretion from stimulated human monocytes or murine leukocytes [IC_{50} (the amount required to inhibit activity by 50%) ~ 1.5 μM] (*4*, *15*). This inhibitor, however, may not be completely selective for ICE and may also inhibit the proteolytic activities of ICE homologs.

To investigate the role of ICE in cytokine release, we examined $ICE^{+/+}$ and $ICE^{-/-}$ monocytes induced by lipopolysaccharide (LPS) and LPS plus nigericin. LPS is a bacterial endotoxin that induces monocytes to produce several cytokines including IL-1β, IL-1α, tumor necrosis factor–α (TNF-α), and IL-6. Nigericin is a K^+-H^+ ionophore that alters K^+ homeostasis and activates a plasma membrane adenosine triphosphatase (ATPase). Nigericin treatment after LPS stimulation enhances processing of the IL-1β precursor and export of mature 17-kD IL-1β from murine and human monocytes (*16*). In $ICE^{+/+}$ monocytes, LPS stimulated IL-1β export into the medium (39 ± 28 pg/ml) and LPS plus nigericin treatment significantly enhanced IL-1β export (140 ± 72 pg/ml, $P < 0.02$) (Table 1). In contrast, $ICE^{-/-}$ monocytes did not release any detectable IL-1β after stimulation with LPS or LPS plus nigericin, and no processed IL-1β was detectable in cell lysates from these cultures (Table 1). This observation establishes the critical role of ICE in processing and export of mature IL-1β.

Treatment with LPS and LPS plus nigericin also enhanced IL-1α release by $ICE^{+/+}$ monocytes (318 ± 186 pg/ml, $P < 0.02$) (Table 1). IL-1α binds to the same cellular receptors as IL-1β (*1*) and is also synthesized as a precursor, but pre–IL-1α is not a substrate for ICE (*3*). Surprisingly, $ICE^{-/-}$ monocytes did not release IL-1α after treatment with LPS plus nigericin, although the intracellular concentration of this cytokine was substantial (115 ± 38 pg/ml). These results implicate ICE as a mediator of IL-1α release from monocytes. Export of IL-1β and IL-1α may involve a common molecular assembly (*17*). For example, ICE may associate with the nigericin-stimulated K^+,H^+-ATPase for transport of IL-1α and

Table 1. Cytokine secretion by adherent monocytes from $ICE^{+/+}$ and $ICE^{-/-}$ mice. Adherent monocytes were isolated from $ICE^{+/+}$ and $ICE^{-/-}$ mice and treated as in (*29*). Cytokines were quantitated in supernatants or cell lysates by an ELISA specific for murine IL-1β, IL-1α, TNF-α, and IL-6. The IL-1α ELISA recognizes both precursor and processed forms. The IL-1β ELISA is highly specific for mature IL-1β and shows <0.2% cross-reactivity against the murine IL-1β precursor.

Cytokine	Stimulus	Supernatant (S) or cell lysate (L)	Cytokine concentration (pg/ml)	
			$ICE^{+/+}$	$ICE^{-/-}$
IL-1β	None	S	0	0
	LPS	S	39 ± 28	0
		L	46 ± 46	0
	LPS + nigericin	S	140 ± 72	0
		L	52 ± 35	0
IL-1α	None	S	0	0
	LPS	S	117 ± 76	10 ± 13
		L	272 ± 175	100 ± 47
	LPS + nigericin	S	318 ± 186	0
		L	201 ± 163	115 ± 38
TNF-α	None	S	0	0
	LPS	S	531 ± 94	318 ± 10
IL-6	None	S	0	0
	LPS	S	2387 ± 190	1032 ± 803

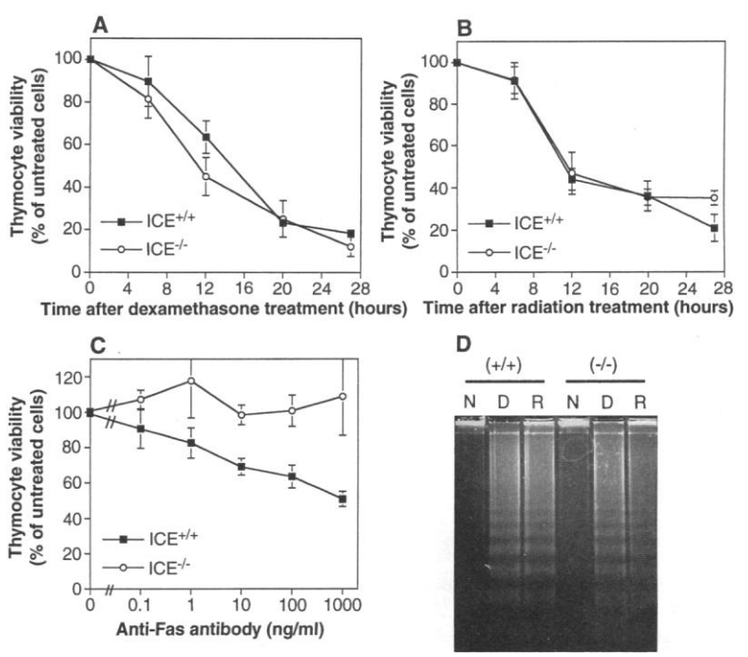

Fig. 2. Apoptosis in thymocytes from $ICE^{+/+}$ and $ICE^{-/-}$ mice. Thymocytes were treated with 1 μM dexamethasone (Sigma) (**A**); 500 cGy of ionizing radiation (**B**); or a hamster antibody to murine Fas (Pharmingen, San Diego) (**C**). Thymocytes were isolated from 5- to 6-week old mice and cultured at a cell density of 10^6 cells per milliliter in 24-well plates. Cells were incubated at 37°C and sampled for viability measurement at the time points indicated. For anti-Fas treatment, cells were incubated for 24 hours with antibody at the concentrations indicated. Cell viability was determined by trypan blue exclusion. Values represent the average viability from three independent wells (± SD) and are normalized to the percentage of viable cells remaining in the untreated cultures. Two independent experiments showed similar results. (**D**) Agarose gel electrophoresis of total DNA from thymocytes that received no treatment (N), or that were treated with 1 μM dexamethasone (D) or 500 cGy ionizing radiation (R). Genomic DNA was isolated from 10^6 thymocytes after 10 hours and subjected to electrophoresis.

K. Kuida and R. A. Flavell, Howard Hughes Medical Institute and Section of Immunobiology, Yale University School of Medicine, New Haven, CT 06510, USA.
J. A. Lippke, G. Ku, M. W. Harding, D. J. Livingston, M. S.-S. Su, Vertex Pharmaceuticals Incorporated, Cambridge, MA 02139, USA.
*To whom correspondence should be addressed.

IL-1β through the plasma membrane. Alternatively, ICE may interact with or activate other proteins, such as calpain (*18*), that may be involved in IL-1α processing and secretion. In contrast to IL-1α, TNF-α and IL-6 are secreted by $ICE^{-/-}$ monocytes, albeit at reduced levels (Table 1).

Overexpression of ICE or its homologs can induce apoptosis in cultured cells (*7, 8*). To determine if normal intracellular concentrations of ICE mediate apoptosis, we investigated the response of $ICE^{-/-}$ thymocytes to three apoptotic stimuli: glucocorticoid (*19*), ionizing radiation, and anti-Fas antibody (*20*). The Fas antigen is a cell surface protein in the TNF-α receptor superfamily that mediates apoptosis in activated T cells (*21, 22*). Fas is encoded by the gene responsible for a lymphoproliferative disorder (*lpr*) in mice. Mice that carry mutations in Fas develop lymphadenopathy and suffer from a systemic autoimmune disease (*23*). Thymocytes isolated from $ICE^{-/-}$ and $ICE^{+/+}$ mice were sensitive to dexamethasone- or radiation-induced apoptosis, as evaluated by cell viability and DNA fragmentation (Fig. 2). A monoclonal antibody to Fas triggered apoptosis in $ICE^{+/+}$ thymocytes in a dose-dependent manner, but did not induce apoptosis in $ICE^{-/-}$ thymocytes (Fig. 2). Analysis of $ICE^{+/+}$ and $ICE^{-/-}$ thymocytes by fluorescence-activated cell sorting (FACS) revealed no differences in expression of cell surface Fas antigen (Fig. 3). We also observed that a potent ICE inhibitor, Cbz-Val-Ala-Asp-(OEthyl)-[(2,6-dichlorobenzoyl)oxy]methyl-ketone, prevented Fas-triggered apoptosis of $ICE^{+/+}$ thymocytes in a dose-dependent manner (*24*).

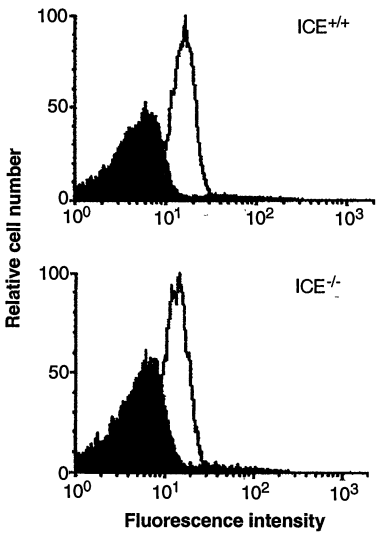

Fig. 3. Expression of Fas on $ICE^{+/+}$ and $ICE^{-/-}$ thymocytes. Cells (10^6) were stained first with 1 μg of the hamster antibody against murine Fas and then with a fluorescein isothiocyanate–conjugated goat antibody to hamster immunoglobulin G (E-Y Laboratories, San Mateo, California). Fas expression on the cell surface was analyzed by FACS. Shaded areas represent staining by the second antibody.

These results establish a role for ICE in Fas-mediated apoptosis of normal thymocytes. Glucocorticoid- and radiation-induced apoptosis of thymocytes presumably occur through different pathways that may involve intracellular serine proteases (*25*). The existence of multiple apoptotic pathways in thymocytes has been inferred previously from studies of mice deficient in Bcl-2. Mature T cells from *bcl-2*$^{-/-}$ mice showed increased sensitivity to apoptosis induced by glucocorticoids and ionizing radiation, but reduced sensitivity to apoptosis stimulated by an antibody to CD3 (*26*). Targeted expression of Bcl-2 in murine cortical ($CD4^+CD8^+$) thymocytes inhibited apoptosis induced by glucocorticoid, ionizing radiation, and anti-CD3, but did not inhibit negative selection of T cells (*27*). Similarly, the tumor suppressor protein p53 mediates apoptosis induced by ionizing radiation and etoposide, but not apoptosis induced by glucocorticoid and other stimuli (*28*).

Unlike the *lpr/lpr* mutation at the murine Fas locus (*23*), disruption of the ICE gene does not lead to autoimmune pathologies in mice within the first 16 weeks of life. This suggests that $ICE^{-/-}$ mice undergo normal clonal deletion of T cells recognizing endogenous superantigens. Given that interaction of Fas and its ligand is involved in programmed cell death after T cell activation (*22*), clonal deletion might be dependent on ICE homologs and their function in apoptotic pathways.

REFERENCES AND NOTES

1. C. A. Dinarello, *FASEB J.* **8**, 1314 (1994).
2. P. E. Auron *et al.*, *Proc. Natl. Acad. Sci. U.S.A.* **81**, 7907 (1984).
3. R. A. Black, S. R. Kronheim, P. R. Sleath, *FEBS Lett.* **247**, 386 (1989); P. R. Sleath, R. C. Hendrickson, S. R. Kronheim, C. J. March, R. A. Black, *J. Biol. Chem.* **265**, 14526 (1990); A. D. Howard *et al.*, *J. Immunol.* **147**, 2964 (1991).
4. N. A. Thornberry *et al.*, *Nature* **356**, 768 (1992).
5. K. A. Wilson *et al.*, *ibid.* **370**, 270 (1994); N. P. C. Walker *et al.*, *Cell* **78**, 343 (1994).
6. J. Yuan, S. Shaham, S. Ledoux, H. M. Ellis, H. R. Horvitz, *Cell* **75**, 641 (1993).
7. L. Wang, M. Miura, L. Bergeron, H. Zhu, J. Yuan, *ibid.* **78**, 739 (1994); S. Kumar, M. Kinoshita, M. Noda, N. G. Copeland, N. A. Jenkins, *Genes Dev.* **8**, 1613 (1994); T. Fernandes-Alnemri, G. Litwack, E. S. Alnemri, *J. Biol. Chem.* **269**, 30761 (1994); C. Faucheu *et al.*, unpublished data.
8. M. Miura, H. Zhu, R. Rotello, E. A. Hartwieg, J. Yuan, *Cell* **75**, 653 (1993).
9. D. L. Vaux, I. L. Weissman, S. K. Kim, *Science* **258**, 1955 (1992).
10. C. A. Ray *et al.*, *Cell* **69**, 597 (1992).
11. V. Gagliardini *et al.*, *Science* **263**, 826 (1994).
12. K. R. Thomas and M. R. Capecchi, *Cell* **51**, 503 (1987).
13. A 2.5-kb Eco RI–Hind III fragment containing ICE exons 4 to 6 and a 1.3-kb Eco RI–Sma I fragment containing exons 8 to 10 (*30*) were subcloned with the neomycin resistance (*neo*) gene cassette (*25*) into a thymidine kinase (*tk*) gene-expressing plasmid to generate the targeting vector. The vector was linearized and introduced into D3 ES cells by electroporation. Sixty-three clones resistant to G418 (300 μg/ml) and gancyclovir (2 μM) were screened by PCR using an exon 10 primer (5′-GTACATAAGAATGAACTGGA-3′) and a *neo* cassette-specific primer (5′-TGCTAAAGCGCATGCTCCAGACTG-3′). One correctly targeted clone was confirmed by Southern blot analysis. Chimeric mice were generated from the mutant ES cell, and heterozygous mice ($ICE^{+/-}$) were interbred to obtain homozygous $ICE^{-/-}$ mice. Expression of ICE mRNA in $ICE^{+/+}$ and $ICE^{-/-}$ mice was analyzed by RT-PCR analysis using the following pairs of PCR primers: (i) ICE complementary DNA (cDNA)–specific primers for exon 3 (5′-GATTCTAAAGGAGGACATCC-3′) and exon 10 (5′-GTACATAAGAATGAACTGGA-3′) to generate an expected PCR product of 930 base pairs (bp); (ii) mutated ICE cDNA-specific primers of exon 3 and a 3′ region of the *neo* cassette (5′-GGGCCAGCTCATTCCTCCACT-3′) to generate an expected PCR product of 700 bp; and (iii) β-actin–specific primers (5′-CACCCTGTGCTGCTCACCGAGGCC-3′) and (5′-CCACACAGATGACTTGCGCTCAGG-3′) to generate an expected product of 700 bp. RT-PCR products were identified with DNA ladder markers of 123 bp (Gibco, Gaithersburg, MD).
14. R. A. Black *et al.*, *J. Biol. Chem.* **263**, 9437 (1988); D. J. Hazuda, J. Strickler, F. Kueppers, P. L. Simon, P. R. Young, *ibid.* **265**, 6318 (1990).
15. S. M. Molineaux *et al.*, *Proc. Natl. Acad. Sci. U.S.A.* **90**, 1809 (1993).
16. D. Perregaux *et al.*, *J. Immunol.* **149**, 1294 (1992); D. Perregaux and C. A. Gabel, *J. Biol. Chem.* **269**, 15195 (1994).
17. W. M. Siders, J. C. Klimovitz, S. B. Mizel, *J. Biol. Chem.* **268**, 22170 (1993).
18. Y. Kobayashi *et al.*, *Proc. Natl. Acad. Sci. U.S.A.* **87**, 5548 (1990); L. M. Carruth, S. Demczuk, S. B. Mizel, *J. Biol. Chem.* **266**, 12162 (1991).
19. J. J. Cohen and R. C. Duke, *J. Immunol.* **132**, 38 (1984).
20. J. Ogasawara *et al.*, *Nature* **364**, 806 (1993).
21. N. Itoh *et al.*, *Cell* **66**, 233 (1991).
22. S.-T. Ju, H. Cui, D. J. Panka, R. Ettinger, A. Marshak-Rothstein, *Proc. Natl. Acad. Sci. U.S.A.* **91**, 4185 (1994); J. Dhein, H. Walczak, C. Baumler, K.-M. Debatin, P. H. Krammer, *Nature* **373**, 438 (1995); T. Brunner *et al.*, *ibid.*, p. 441; S.-T. Ju *et al.*, *ibid.*, p. 444.
23. R. Watanabe-Fukunaga, C. I. Brannan, N. G. Copeland, N. A. Jenkins, S. Nagata, *Nature* **356**, 314 (1992).
24. The $ICE^{+/+}$ thymocytes were incubated with 1 μg/ml anti-Fas antibody in the presence of 0.1, 1.0, or 10.0 μM of Cbz-Val-Ala-Asp-(OEthyl)-[(2,6-dichlorobenzoyl)oxy]methyl-ketone. Thymocyte viability was assessed 24 hours after treatment as in Fig. 2. Inhibition of apoptosis ($IC_{50} \sim 1$ μM) was determined in two independent experiments.
25. V. M. Weaver, B. Lach, P. R. Walker, M. Sikorska, *Biochem. Cell. Biol.* **71**, 488 (1993); C. Voelkel-Johnson, A. J. Entingh, W. S. M. Wold, L. R. Gooding, S. M. Laster, *J. Immunol.* **154**, 1707 (1995).
26. K.-i. Nakayama *et al.*, *Science* **261**, 1584 (1993); D. J. Vels, C. M. Sorenson, J. R. Shutter, S. J. Korsmeyer, *Cell* **75**, 229 (1993).
27. C. L. Sentman, J. R. Shutter, D. Hockenbery, O. Kanagawa, S. J. Korsmeyer, *Cell* **67**, 879 (1991).
28. L. W. Lowe, E. M. Schmitt, S. W. Smith, B. A. Osborne, T. Jacks, *Nature* **362**, 847 (1993); A. R. Clarke *et al.*, *ibid.* p. 849.
29. Cell suspensions were prepared from spleens excised from $ICE^{+/+}$ or $ICE^{-/-}$ mice. Adherent monocytes were stimulated for 16 to 18 hours with 1 μg/ml phenol-extracted LPS (*Escherichia coli* strain 0111:B4; Sigma), and supernatants were harvested for quantitation of IL-1β. Cells from some cultures were washed once, incubated with 10 μM nigericin for an additional 30 min, and the supernatants harvested again. Viability of monocytes after nigericin stimulation was >98% as measured by trypan blue staining or lactate dehydrogenase activity in culture supernatants, indicating that minimal cytolysis had occurred during the experiment. IL-1β was quantitated in supernatants and cell lysates with an enzyme-linked immunosorbent assay (ELISA) specific for mature murine IL-1β (PerSeptive Diagnostics,

Cambridge, MA). We determined the specificity by testing the reactivity of purified recombinant murine IL-1β precursor in the ELISA. At concentrations of 20 pg/ml and 10 ng/ml, respectively, mature IL-1β and precursor IL-1β were recognized equally, indicating a cross-reactivity of 0.2%. The IL-1α antibody was from Genzyme (Cambridge, MA), and the TNF-α and IL-6 antibodies were from Biosource International (Camarillo, CA).
30. F. J. Casano, A. M. Rolando, J. S. Mudgett, S. M. Moleneaux, *Genomics* **20**, 474 (1994).
31. We thank K. Hsiao, R. Aldape, and J. Partaledis for help with gene cloning; J. Elsemore, C. Hughes, and D. Butkis for help with gene targeting; L. Lauffer and T. Faust for help with ELISA of cytokines; M. Fleming for oligonucleotide synthesis; D. Y. Loh for providing the *neo* and *tk* gene cassettes; and J. Boger and V. Sato for critical reading and discussion of the manuscript. R.A.F. and K.K. are supported by the Howard Hughes Medical Institute.

25 January 1995; accepted 2 March 1995

Requirement for Phosphatidylinositol-3 Kinase in the Prevention of Apoptosis by Nerve Growth Factor

Ryoji Yao and Geoffrey M. Cooper*

Nerve growth factor (NGF) induces both differentiation and survival of neurons by binding to the Trk receptor protein tyrosine kinase. Although Ras is required for differentiation, it was not required for NGF-mediated survival of rat pheochromocytoma PC-12 cells in serum-free medium. However, the ability of NGF to prevent apoptosis (programmed cell death) was inhibited by wortmannin or LY294002, two specific inhibitors of phosphatidylinositol (PI)-3 kinase. Moreover, platelet-derived growth factor (PDGF) prevented apoptosis of PC-12 cells expressing the wild-type PDGF receptor, but not of cells expressing a mutant receptor that failed to activate PI-3 kinase. Cell survival thus appears to be mediated by a PI-3 kinase signaling pathway distinct from the pathway that mediates differentiation.

Apoptosis plays a key role in the normal development of the nervous system. Up to 50% of many types of developing neurons are eliminated by apoptosis (*1*). The survival of developing neurons is dependent on specific neurotrophic factors secreted by their target cells. NGF is the prototype of this family of neurotrophins, which also includes brain-derived neurotrophic factor, neurotrophin-3, and neurotrophin-4 (*2*). NGF induces both cell differentiation and survival by binding to the Trk receptor protein tyrosine kinase (*3*). In rat pheochromocytoma PC-12 cells, neurite outgrowth is induced by activation of a signaling pathway that includes the Ras guanine nucleotide–binding protein and the protein kinases, Raf and mitogen-activated protein (MAP) kinase (*4*, *5*). NGF also prevents apoptosis of PC-12 cells in serum-free medium (*6*), but the signaling pathway that promotes cell survival has not been identified. Here, we report that prevention of apoptosis by NGF is independent of Ras but requires the activity of PI-3 kinase.

We first investigated whether prevention of apoptosis by NGF was dependent on Ras signaling. PC-12 cells in serum-free medium underwent apoptosis (*6*), as indicated by characteristic internucleosomal DNA fragmentation, starting at 3 hours and continuing for 24 hours after serum deprivation. Apoptosis was prevented by NGF, epidermal growth factor (EGF), or insulin, all of which activate receptors that are protein tyrosine kinases (Fig. 1). To determine whether Ras was required for the inhibition of apoptosis, we used a PC-12 cell line (M-M17-26) that expresses the dominant inhibitory mutant RasN17, which interferes with normal Ras function (*7*). RasN17 expression in this cell line effectively inhibits Raf activation and neuronal differentiation in response to NGF (*5*). Activation of MAP kinase was similarly inhibited by RasN17 expression (Fig. 1A). In contrast, the expression of RasN17 in these cells did not interfere with the ability of NGF, EGF, or insulin to prevent apoptosis (Fig. 1B). Similar results were obtained with two additional subclones of PC-12 cells that expressed RasN17. It therefore appears that cell survival, but not cell differentiation, is mediated by a Ras-independent signaling pathway. Ras is similarly not required for NGF-mediated survival of sympathetic neurons (*8*).

In addition to Ras, the signaling molecules activated by protein tyrosine kinases include phospholipase C-γ (PLC-γ) and PI-3 kinase (*9*). PLC-γ catalyzes the hydrolysis of PI-4,5-bisphosphate (PIP_2), which yields diacylglycerol and inositol triphosphate and results in the activation of protein kinase C. Because direct activation of protein kinase C by the phorbol ester 12-O-tetradecanoylphorbol-13-acetate (TPA) failed to inhibit apoptosis (*6*) (Fig. 1), participation of PLC-γ in a signaling pathway that promotes cell survival seems unlikely. On the other hand, phosphorylation of PIP_2 by PI-3 kinase yields PI-3,4,5-trisphosphate (PIP_3), the function of which has not been established (*10*). PI-3 kinase is activated by various receptor protein tyrosine kinases, including Trk (*11*). Although Ras may contribute to its activation, PI-3 kinase also appears to be activated by Ras-independent pathways (*12*). We therefore investigated the possible role of PI-3 kinase in signaling pathways that promote cell survival.

Wortmannin inhibits PI-3 kinase both in vitro and in vivo (*13*). Addition of wortmannin to cells maintained in NGF induced a pattern of DNA fragmentation characteristic of apoptosis within 3 hours (Fig. 2A); this time course is similar to that of apoptosis induced by serum deprivation (*6*). The intensity of DNA fragmentation

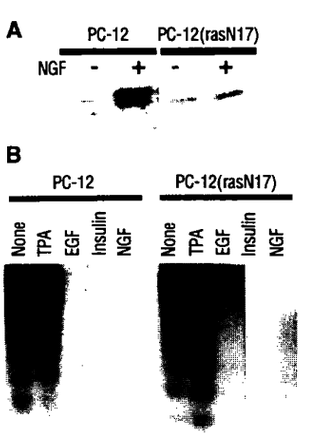

Fig. 1. Inhibition of apoptosis by growth factors is independent of Ras function. (**A**) Inhibition of MAP kinase activation by RasN17 expression. Normal PC-12 cells or M-M17-26 cells expressing the dominant inhibitory RasN17 mutant [PC-12 (rasN17)] (*5*) were incubated without (−) or with (+) NGF (100 ng/ml) for 5 min. Total cell lysates (20 μg of protein) were separated by SDS–polyacrylamide gel electrophoresis, and MAP kinase activity was determined by an in-gel assay using myelin basic protein as the substrate (*27*). (**B**) Inhibition of apoptosis by growth factors. Cells were plated on 100-mm culture dishes (2×10^6 cells per dish) in DMEM supplemented with fetal bovine serum (5%) and horse serum (10%). After 3 days, cells were washed five times with serum-free DMEM and were cultured in the presence of no additives (None), TPA (200 nM), EGF (100 ng/ml), insulin (5 μM), or NGF (100 ng/ml). After 24 hours, the cells attached to the culture dish and those suspended in the medium were collected by centrifugation. Soluble cytoplasmic DNAs were extracted (*28*), separated by electrophoresis in 1.8% agarose gels, blotted onto GeneScreen Plus membrane (NEN-DuPont, Boston, Massachusetts), and hybridized with ^{32}P-labeled, Eco RI–digested rat genomic DNA as a probe.

Division of Molecular Genetics, Dana-Farber Cancer Institute and Department of Pathology, Harvard Medical School, Boston, MA 02115, USA.

*To whom correspondence should be addressed.